
# Department of Computer Science and Engineering

# CSE 597

## Inter Distance Measurement of Sensor by Time Difference of Arrival of Signals

**Submitted by**

**Jihan Sultana**

**ID : 2015-1-96-001**

**Supervised By**

**Dr. Anisur Rahman**

**Assistant Professor**

# Department of Computer Science and Engineering

**EAST WEST UNIVERSITY**

# Chapter 1

# Introduction

Wireless sensor networks (WSNs) are a significant technology attracting considerable research interest. Recent advances in wireless communications and electronics have enabled the development of low-cost, low-power and multi-functional sensors that are small in size and communicate in short distances. Cheap, smart sensors, networked through wireless links and deployed in large numbers, provide unprecedented opportunities for monitoring and controlling homes, cities, and the environment.

In addition, networked sensors have a broad spectrum of applications in the defense area, generating new capabilities for reconnaissance and surveillance as well as other tactical applications [1]. Self-localization capability is a highly desirable characteristic of wireless sensor networks. In environmental monitoring applications such as bush fire surveillance, water quality monitoring and precision agriculture, the measurement data are meaningless without knowing the location from where the data are obtained. Moreover, location estimation may enable a myriad of applications such as inventory management, intrusion detection, road traffic monitoring, health monitoring, reconnaissance and surveillance.

Sensor network localization algorithms estimate the locations of sensors with initially unknown location information by using knowledge of the absolute positions of a few sensors and inter-sensor measurements such as distance and bearing measurements. Sensors with known location information are called anchors and their locations can be obtained by using a global positioning system (GPS), or by installing anchors at points with known coordinates. In applications requiring a global coordinate system, these anchors will determine the location of the sensor network in the global coordinate system. In applications where a local coordinate system suffices (e.g., smart homes), these anchors define the local coordinate system to which all other sensors are referred. Because of constraints on the cost and size of sensors, energy consumption, implementation environment (e.g., GPS is not accessible in some environments) and the

deployment of sensors (e.g., sensor nodes may be randomly scattered in the region), most sensors do not know their locations. These sensors with unknown location information are called non-anchor nodes and their coordinates will be estimated by the sensor network localization algorithm.

However, location discovery in wireless sensor networks is very challenging. First the algorithm positioning must be distributed and localized in order to scale well for large sensor networks. Second, the localization protocol must minimize communication and computation overhead for each sensor since nodes have very limited resources (power, CPU, memory, etc.). Third, the positioning functionality should not increase the cost and complexity of the sensor since an application may require thousands of sensors. Fourth, a location detection scheme should be robust. It should work with accuracy and precision in various environments, and should not depend on sensor to sensor connectivity in the network. The TPS positioning scheme proposed in this research is designed to meet these challenges.

The major contribution of this paper is twofold. First, we propose a time-based location detection scheme for outdoor sensor networks and demonstrate our algorithm by simulation. Second, we analyze the theoretical performance of our scheme in noisy environments and identify possible sources of error with measures to help mitigate them. We put very few restrictions on the network layout and propose a scheme suitable for general outdoor sensor networks. We rely on RF signal, which performs well compared to ultrasound, infrared, etc., in outdoor environments [29]. We measure the difference in arrival times (TDoA) of beacon signals. In previous research, Timeof-Arrival (ToA) has proven more useful than RSSI in location determination [32]. TPS does not need the specialized antennae generally required by an Angle of Arrival **(AoA)** positioning system. This time-based location detection scheme avoids the drawbacks of many existing systems for outdoor sensor location detection. Our simulations show that TPS is potentially very effective and computationally efficient. Compared to existing schemes proposed in the context of outdoor sensor networks, our scheme bas the following characteristics and advantages:

- Time synchronization of all base stations and nodes is not required in TPS. Sensors measure the difference in signal arrival times using a local clock. Base stations schedule their transmissions based on receipt of other beacon transmissions and do not require synchronized clocks. Many existing location discovery systems for Sensor networks require time synchronization among base stations [25], or between satellites and sensors [15]. Impact time synchronization can degrade the positioning accuracy.

- There are no requirements for ultrasound receiver [8], [32], second radio [15] or specialized antennae [ 5] **,**[2], [25] at base stations or sensors. Our scheme does not incur the complexity, power consumption and cost associated with these components. (TPS sensors do require the ability to measure the difference in signal arrival times with precision.)

- Our algorithm is not iterative-and doesn't require a complicated refinement step as does [28], [31],[33].We refine position estimates by averaging time difference measurements over several beacon intervals prior to calculating position. This is useful to mitigate the effects of momentary interference and fast fading. This averaging requires less computation than repeatedly solving linear system matrices, least squares or multilateration algorithms.

- TPS has or low multilateration computation algorithms cost. Our location detection algorithm is based on simple algebraic operations on scalar values. On the other hand, multilateration based systems[15],[17],[32],[33] require matrix operations to optimize the objective functions (minimum mean square estimation or maximum likelihood estimation), which induces higher computation overhead at each sensor.

- Sensors listen passively each and are not required to make radio transmissions. Base stations transmit all the beacon signals. This conserves sensor energy and reduces RF

channel use. Connectivity based systems often require global flooding [26] or global connectivity information [35] to estimate range.

# Chapter 2

# Measurement techniques

Measurement techniques in WSN localization can be broadly classified into three categories: Angle-of-arrival (AOA) measurements, distance related measurements and RSS profiling techniques.

## 2.1. Angle-of-arrival measurements

The angle-of-arrival measurement techniques can be further divided into two subclasses: those making use of the receiver antenna's amplitude response and those making use of the receiver antenna's phase response.

Beam forming is the name given to the use of anisotropy in the reception pattern of an antenna, and it is the basis of one category of AOA measurement techniques. The measurement unit can be of small size in comparison with the wavelength of the signals. The beam pattern of a typical anisotropic antenna is shown in Fig. 1. One can imagine that the beam of the receiver antenna is rotated electronically or mechanically, and the direction corresponding to the maximum signal strength is taken as the direction of the transmitter. Relevant parameters are the sensitivity of the receiver and the beam width. A technical problem to be faced and overcome arises when the transmitted signal has a varying signal strength. The receiver cannot differentiate the signal strength variation due to the varying amplitude of the transmit ted signal and the signal strength variation caused by the anisotropy in the reception pattern. One approach to dealing with the problem is to use a second non-rotating and omnidirectional antenna at the receiver. By normalizing the signal strength received by the rotating anisotropic antenna with respect to the signal strength received by the non-rotating omnidirectional antenna, the impact of varyisng signal strength can be largely removed.

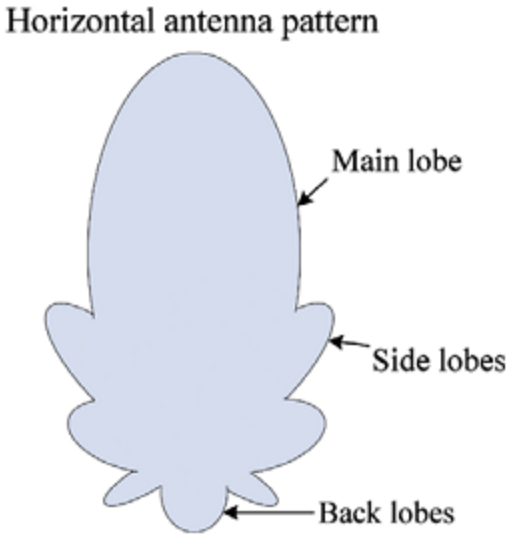


**Fig. 1. An illustration of the horizontal antenna pattern of a typical anisotropic antenna.**

Another widely used approach [6] to cope with the varying signal strength problem is to use a minimum of two (but typically at least four) stationary antennas with known, anisotropic antenna patterns. Overlapping of these patterns and comparing the signal strength received from each antenna at the same time yields the transmitter direction, even when the signal strength changes. Coarse tuning is performed by measuring which antenna has the strongest signal, and it is followed by fine tuning which compares amplitude responses. Because small errors in measuring the received power can lead to a large AOA measurement error, a typical measurement accuracy for four antennas is $10–15^0$. With six antennas, this can be improved to about $5^0$, and $2^0$ with eight antennas [6].

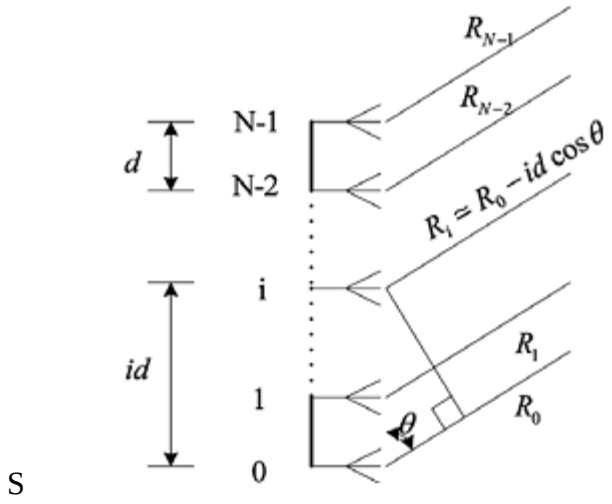


**Fig. 2. An antenna array with N antenna elements.**

The second category of measurement techniques, known as phase interferometry [7], derives the AOA measurements from the measurements of the phase differences in the arrival of a wave front. It typically requires a large receiver antenna (relative to the wavelength of the transmitter signal) or an antenna array. Fig. 2 shows an antenna array of N antenna elements. The adjacent antenna elements are separated by a uniform distance d. The distance between a transmitter far away from the antenna array and the ith antenna element can be approximated by

$$R \approx R_0 - id\cos\theta$$

where $R_0$ is the distance between the transmitter and the 0th antenna element and $\theta$ is the bearing of the transmitter with respect to the antenna array. The transmitter signals received by adjacent antenna elements have a phase difference of $2\pi\frac{dcos\theta}{\lambda}$, which allows us to obtain the bearing of the transmitter from the measurement of the phase difference. This works quite well for high SNR but may fail in the presence approach of strong co-channel interference and/or multipath signals [7].

The accuracy of AOA measurements is limited by the directivity of the antenna, by shadowing and by multipath reflections. How to obtain accurate AOA measurements in the presence of

multipath and shadowing errors has been a subject of intensive research. AOA measurements rely on a direct line-of-sight (LOS) path from the transmitter to the receiver. However a multipath component may appear as a signal arriving from an entirely different direction and can lead to very large errors in AOA measurements. Multipath problems in AOA measurements can be addressed by using the maximum likelihood (ML) algorithms[7]. Different ML algorithms have been proposed in the literature which make different assumptions about the statistical characteristics of the incident signals[8–10]. They can be classified into deterministic and stochastic ML methods. Typically ML methods will estimate the AOA of each separate path in a multipath environment. The implementation of these methods is computationally intensive and requires complex multidimensional search. The dimensionality of the search is equal to the total number of paths taken by all the received signals [7]. The problem is further complicated by the fact that the total num ber of paths is not known a priori and must be estimated. Different from the earlier ML methods, which assume the incoming signal is an unknown stochastic process, another class of ML methods [11],[12],[13] assume that the structure of the signal waveform is known to the receiver. This assumption is possible in some digital communication systems because the modulation format is known to the receiver and many systems are equipped with a known training sequence in the preamble. This extra information is exploited to improve the accuracy of AOA measurements or simplify computation.

Yet another class of AOA measurement methods is based on so-called subspace-based algorithms[14],[21],[16],[24]. The most well known methods in this category are MUSIC (multiple signal classification) [14] and ESPRIT (estimation of signal parameters by rotational invariance techniques). These eigenanalysis based direction finding algorithms utilize a vector space formulation, which takes advantage of the underlying parametric data model for the sensor array problem. They require a multi-array antenna in order to form a correlation matrix using signals received by the array. The measured signal vectors received at the M array elements is visualized as a vector in M dimensional space. Utilizing an eigen-decomposition of the correlation matrix, the vector space is separated into signal and noise subspaces. Then the MUSIC algorithm searches for nulls in the magnitude squared of the projection of the direction vector onto the noise subspace. The nulls are a function of angle-of-arrival, from which angle-of-

arrival can be estimated. For linear arrays, Root-MUSIC [18], a polynomial rooting version of MUSIC, improves the resolution capabilities of MUSIC. A weighted norm version of MUSIC, WMUSIC [19], also gives an extension in the resolution capabilities compared to the original MUSIC. ESPRIT [21] [16] is based on the estimation of signal parameters via rotational invariance techniques. It uses two displaced sub arrays of matched sensor doublets to exploit an underlying rotational invariance among signal subspaces for such an array. A comprehensive experimental evaluation of MUSIC, Root-MUSIC, WMUSIC, Min-Norm [20] and ESPRIT algorithms can be found in A very large number of AOA measurement techniques have been developed which are based on MUSIC and ESPRIT, to cite but two, see e.g. [24] [22]. Due to space limitations, we do not provide an exhaustive list of them in this paper. Readers may refer to [36] for a detailed technical discussion on AOA measurement techniques.

## 2.2. Distance related measurements

Distance related measurements include propagation time based measurements, i.e., one-way propagation time measurements, roundtrip propagation time measurements and time-difference-of-arrival (TDOA) measurements, and RSS measurements. Another interesting technique measuring distance, which does not fall into the above categories, is the lighthouse approach shown in [43]. In the following paragraphs we provide further details of these techniques.

### *2*.2.1. One-way propagation time and roundtrip propagation time measurements

One-way propagation time and roundtrip propagation time measurements are also generally known as time-of-arrival measurements. Distances between neighboring sensors can be estimated from these propagation time measurements.

One-way propagation time measurements measure the difference between the sending time of a signal at the transmitter and the receiving time of the signal at the receiver. It requires the local time at the transmitter and the local time at the receiver to be accurately synchronized. This

requirement may add to the cost of sensors by demanding a highly accurate clock and/or increase the complexity of the sensor network by demanding a sophisticated synchronization mechanism. This disadvantage makes one-way propagation time measurements a less attractive option than measuring roundtrip time in WSNs. Roundtrip propagation time measurements measure the difference between the time when a signal is sent by a sensor and the time when the signal returned by a second sensor is received at the original sensor. Since the same clock is used to compute the roundtrip propagation time, there is no synchronization problem. The major error source in roundtrip propagation time measurements is the delay required for handling the signal in the second sensor. This internal delay is either known via a priori calibration, or measured and sent to the first sensor to be subtracted. A detailed discussion on circuitry design for roundtrip propagation time measurements can be found in [37].

Time delay measurement is a relatively mature field. The most widely used method for obtaining time delay measurement is the generalized cross-correlation method [38] [27]. A detailed discussion on the cross-correlation method is given in Section 2.2.3.

Based on the observation that the speed of sound in the air is much smaller than the speed of light (RF) in the air, Priyantha et al. developed a technique to measure the one-way propagation time [39], which solved the synchronization problem. It uses a combination of RF and ultrasound hardware.

On each transmission, a transmitter sends an RF signal and an ultrasonic pulse at the same time. The RF signal will arrive at the receiver earlier than the ultrasonic pulse. When the receiver receives the RF signal, it turns on its ultrasonic receiver and listens for the ultrasonic pulse. The time difference between the receipt of the RF signal and the receipt of the ultrasonic signal is used as an estimate of the one-way acoustic propagation time. Their method gave fairly accurate distance estimate at the cost of additional hardware and complexity of the system because ultrasonic reception suffers from severe multipath effects caused by reflections from walls and other objects. A recent trend in propagation time measurements is the use of ultra wide band

(UWB) signals for accurate distance estimation [40][30]. A UWB signal is a signal whose bandwidth to center frequency ratio is larger than 0.2 or a signal with a total bandwidth of more than 500 MHz. UWB can achieve higher accuracy because its bandwidth is very large and therefore its pulse has a very short duration. This feature makes fine time resolution of UWB signals and easy separation of multipath signals possible.

### 2.2.2. Light house approach to distance measurements

Another interesting approach to distance measurements is the lighthouse approach [43] which derives the distance between an optical receiver and a transmitter of a parallel rotating optical beam by measuring the time duration that the receiver dwells in the beam.

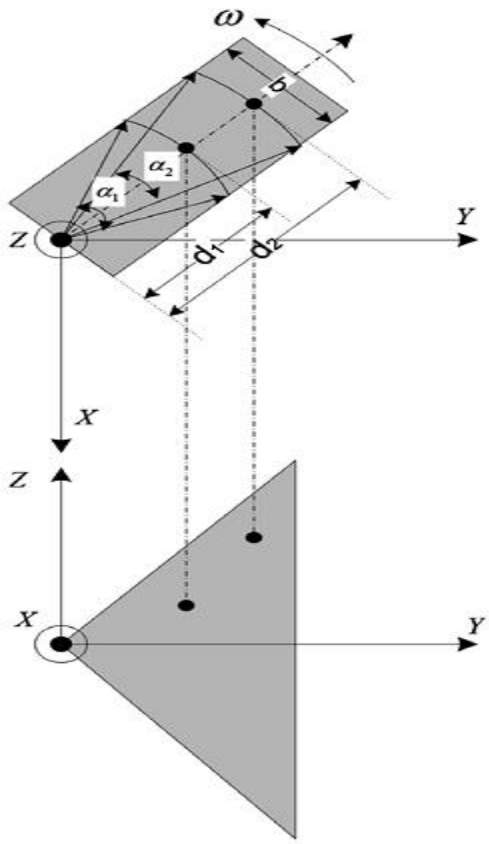


Fig. 3. An illustration of the lighthouse approach for distance measurement.

Fig. 3 is an illustration of the lighthouse approach for distance measurement. A transmitter located at the origin is equipped with a parallel optical beam, i.e., an optical beam whose beam width b is constant with respect to the distance from the rotational axis of the beam.

The optical beam rotates at an unknown angular velocity ω around the Z axis. An optical receiver in the XY plane and at a distance $d_1$ from the Z axis detects the beam for a time duration $t_1$. From Fig. 3, it can be shown that

$$d_1 \approx \frac{b}{2\sin(\alpha_{1/2})} = \frac{b}{2\sin(\omega t_{1/2})}$$

The unknown angular velocity x can be derived from the difference between the time instant when the optical receiver first detects the beam and the time instant when the optical receiver detects the beam for the second time. Therefore the distance$d_1$ can be derived from the time duration $t_1$ that the optical receiver dwells in the beam. The lighthouse approach measures the distance between an optical receiver and the rotational axis of the optical beam generated by the transmitter. A major advantage of the lighthouse approach is the optical receiver can be of a very small size, thus making the idea of ‘‘smart dust’’ possible [43].

However the transmitter may be large. The approach also requires a direct line-of-sight between the optical receiver and the transmitter.

### 2.2.3. Time-difference-of-arrival measurements

There is a category of localization algorithms utilizing TDOA measurements of the transmitter's signal at a number of receivers with known location information to estimate the location of the transmitter.

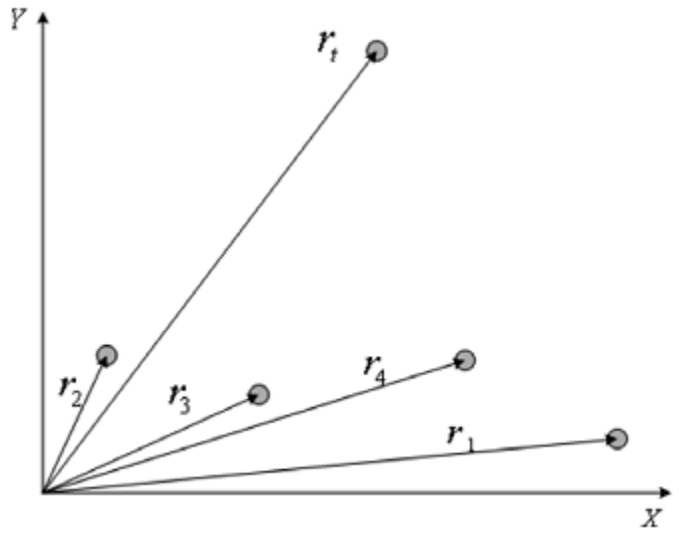


Fig. 4. Localization using time-difference-of-arrival measurement

Fig. 4 shows a TDOA localization scenario with a group of four receivers at locations $r_1$, $r_2$, $r_3$, $r_4$ and a transmitter at $r_t$. The TDOA between a pair of receivers i and j is given by

$$\Delta t_{ij} \triangleq t_i - t_j = \frac{1}{c}\left( \left\| r_i - r_t \right\| - \left\| r_j - r_t \right\| \right), \qquad i \neq j$$

where $t_i$ and $t_j$ are the time when a signal is received at receivers i and j, respectively, c is the propagation speed of the signal, and ||.||denotes the Euclidean norm.

Measuring the TDOA of a signal at two receivers at separate locations is a relatively mature field [41].

The most widely used method is the generalized cross-correlation method, where the cross-correlation function between two signals si and sj received at receivers i and j is given by integrating the lag product of two received signals for a sufficiently long time period T,

$$\rho_{i,j}(\tau) = \frac{1}{T}\int_{O}^{T} s_{i(t)}\, s_{j(t-\tau)}\, dt$$

The cross-correlation function can also be obtained from an inverse Fourier transform of the estimated frequency domain cross-spectral density function. Frequency domain processing is often preferred because the signals can be filtered prior to computation of the cross-correlation function. The cross-correlation approach requires very accurate synchronization among receivers but does not impose any requirement on the signal transmitted by the transmitter. The accuracy and temporal resolution capabilities of TDOA measurements will improve when the separation between receivers increases because this increases differences between time-of-arrival. Closely spaced multiple receivers may give rise to multiple received signals that cannot be separated.

For example, TDOA of multiple signals that are not separated by more than the width of their cross-correlation peaks (whose location on the time-delay axis corresponds to TDOA) usually cannot be resolved by conventional TDOA measurement techniques [42]. Yet another factor affecting the accuracy of TDOA measurement is multipath. Overlapping cross-correlation peaks due to multipath often cannot be resolved. Even if distinct peaks can be resolved, a method must be designed for selecting the correct peak value, such as choosing the largest or the first peak [7]. It is worth noting that Gardner and Chen proposed an approach in [42] [9], which exploits the cyclostationarity property of a certain signal to obtain substantial tolerance to noise and interference. The cyclostationarity property is a direct result of the underlying periodicities in the signal due to periodic sampling, scanning, modulating, multiplexing, and coding operations employed in the transmitter. Both the frequency-shifted and time-shifted cross-correlations are utilized to exploit the unique cyclostationarity property of the signal.

Their method requires the signal of interest to have a known analog frequency or digital keying rate that is distinct from that of the interfering signal.

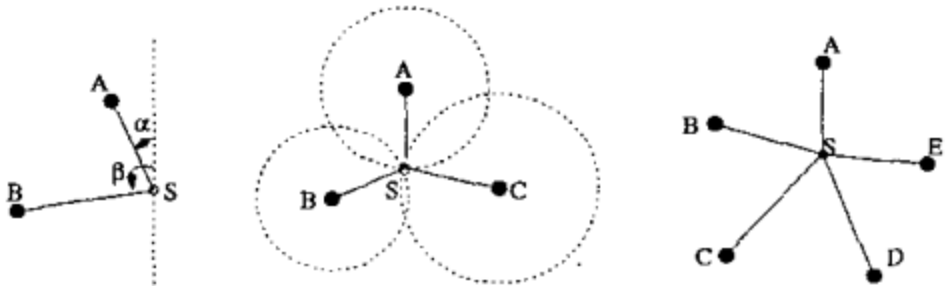


**(i) triangulation (ii) trilateration (iii) multilaterations**

**Fig. 5 Range or angle combining techniques.**

Triangulation, trilateration, and multilateration are the three techniques for combining ranges and angles. Triangulation is the simplest. As in Fig. 5(i), if the angles (α and β*)* to base stations A and B are known, the location of *S* is where lines from A and B intersect. Thus for **AoA,** at least two base stations are required. Trilateration computes the intersection of three circles, as shown in Fig. 5(ii). If the range to each base station is not accurate, the three circles may not have a common intersection point leading to ambiguous solutions. Multilateration uses an objective function to minimize the difference between the estimated position and real position of a sensor. For example in Fig. 5(iii), we can use min $\sum_i (D_{si} - \hat{D}_{Si})^2$ to compute $(x,y)$ for S, where $D_{si} = \sqrt{(x - x_i)^2 + (y - y_i)^2}$, $\hat{D}_{Si}$ is the estimated range from *S* to *i*, *i* = *A*,*B*,C,D,E. This technique can improve accuracy but involves higher computation overhead. For details on multilateration, we refer the readers to [32]. Both trilateration and multilateration require at least 3 base stations. TPS uses trilateration with range difference information. We compute a sensor's position and its range to the master base station at the same time.

### 2.2.4 Existing Sensor Location Detection Schemes

GPS is the most popular localization system but may not be desirable in a sensor network due to cost, form factor, energy consumption, and the requirement for a second radio. GPS-less localization techniques have been researched extensively. For example, Ref. [44] proposes to use the centroid of multiple base stations to approximate the sensor location. In this subsection, we are going to overview in detail several works designed for outdoor sensor networks. For a taxonomy of location systems for ubiquitous computing we refer the readers to [45]Ref. [32]proposes a TDoA based scheme(AHLQS) that requires base stations to transmit both ultrasound and RF signals simultaneously. The RF signal is used for synchronization purposes. A sensor will measure the difference of the arrival times between the two signals and determine the range to the base station. Multilateration is applied to combine range estimates to generate location data. Testbed experiments demonstrate that AHLoS provides fine-grained localization capability. However, ultrasound transceivers can only cover a short range (several meters) and large numbers of base stations may be required to cover large areas. Other contributions by [32] include the introduction of iterative multilateration and collaborative multilateration. In iterative multilateration, a sensor becomes a base station after its position is determined. Whenever a sensor has range estimates to at least three base stations, multilateration is used to compute its position; otherwise, it continues to listen to beacon signals from base stations. If it is impossible for a sensor to find 3 base stations, collaborative multilateration can be used. In collaborative multilateration two or more sensors (which can be multiple hops apart) can form an over determined system of equations with a unique solution set. Feasible conditions for collaborative multilateration are further explored in [33]. Ref. [17] compares the performance of different multilateration methods by simulation and proposes a new and fast iterative improvement algorithm to optimize location discovery. Ref. [8] designs and analyzes an acoustic ranging system for robotics applications and embedded sensor technology. This paper examines methods to detect and eliminate various types of interference.

As mentioned earlier, AoA techniques require special antennae and may not perform well due to omnidirectional multipath reflections. To avoid requirements for directional antennae, Ref. [25] first transforms TDoA measurements in to AoA information and then applies triangulation to compute location. This scheme requires at least 3 base stations with synchronized rotating directional antennae. Non-zero antennae beam width and imperfect synchronization contributes to decrease system accuracy. A prototype navigation system based on AoA measurements for autonomous vehicles is presented in [23]. It estimates AoA by means of a set of optical sources and a rotating optical sensor. This system is not suitable for outdoor sensor networks due to its cost and complexity. Our scheme is similar to the one in Ref. [25] in that TPS measures TDoA at each sensor and has no additional special requirements for sensors. However, we do not use directional antenna in base stations and we do not require any kind of synchronization in the whole network.

The works mentioned above are all based on straight line range estimation to base stations. Ad Hoc positioning system (AI'S) [26] first estimates ranges based on DV-hop, DV-distance, or Euclidean, and then applies trilateration to compute the location of each sensor. If enough base stations are available, location errors for APS with DV-hop can be about 30% of radio range in a dense and regular topology. For sparse and irregular network topologies, the accuracy degrades to roughly the radio range. For DV distance and Euclidcan, the performance of APS also depends on the accuracy of the distance measured between neighboring sensors. Ref. [31] goes one step further: it refines location estimates computed by APS with DV-hop by using neighboring sensor position and distance estimates to help convergence to a better solution. To mitigate error propagation, a confidence weight from 0 to 1 is associated with each estimated position. With measured distance errors of 5% , [31] produces an error of 33% of radio range on average for random graphs. Another work is [33], which uses DV-distance to compute range and Min-Max to compute position. To refine position estimates, [33**]** uses a computation tree. Ref. [46] compares [26], [31], and [33] in simulation.

Locating a subscriber in cellular networks or PCS systems has been well studied in literature [5] The techniques involved produce coarse location granularity (tens or hundreds of meters), thus may not he suitable for outdoor sensor networks. Research on indoor or in-building localization is on-going and many interesting systems have been designed. Examples include Active Badge [36] Active Bat, RADAR, Cricket, and Spot ON, to name a few. Some of these systems require location surveys which are not possible with an air deployed outdoor sensor network. For a brief overview on these systems, we refer the readers to [17]. Other interesting works in sensor networks include [35].

# Chapter 3

## Network Model

We assume that the sensors are deployed randomly over a 2-dimensional monitored area (on the ground). (However, Our proposed sensor positioning scheme can be easily extended to 3-dimensional space.) Each sensor has limited resources (battery, CPU, etc), and is equipped with an omni-directional antenna. Three base stations A, B, C, with known coordinates $(x_a,y_a)$, $(x_b,y_b)$, and $(x_c,y_c)$, respectively, are placed beyond the boundary of the monitored area, as shown in Fig. 6. Let us assume A be the master base station. Assume the monitored area is enclosed within the angle ∠BAC. Let the unknown coordinates of a sensor be $(x, y)$, which will he determined by Time-Based Positioning Scheme (TPS). Each base station can reach all sensors in the monitored area. One restriction on the placement of these base stations is that they must be non-collinear, as otherwise, the sensor locations will be indistinguishable.

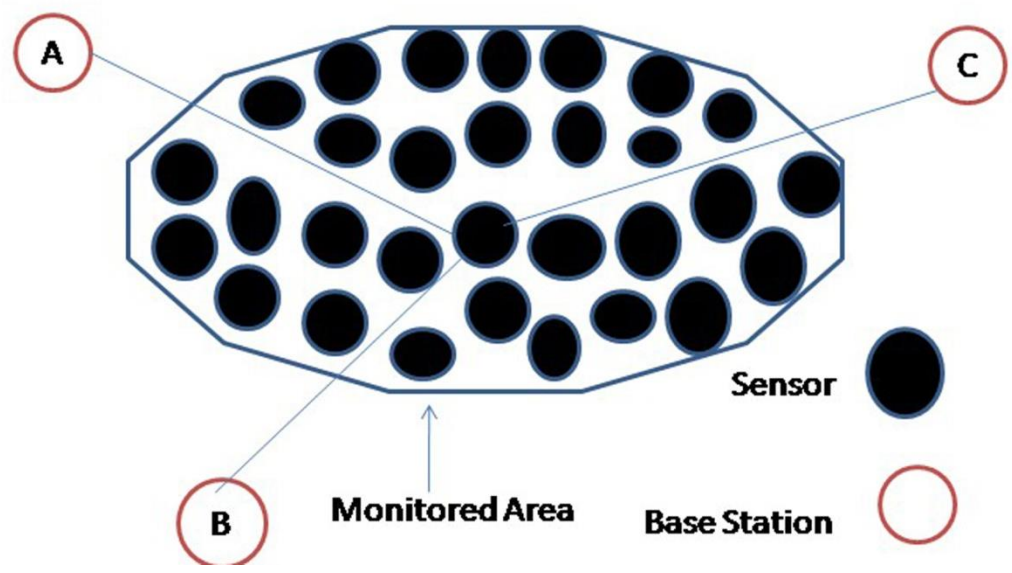


**Fig. 6 An example sensor network**

Note that these base stations will transmit RF beacon signals periodically to assist each sensor with location discovery. They have long-term power supplies and can receive RF signals from each other. Note that there is no time synchronization among these three base stations. However, we require base stations to detect signal arrival times with precision and to accurately calculate total turnaround delay. This calculated turn-around delay consists of a random delay combined with known system transmission and reception delays.

**Remark:** If the monitored area is so large that 3 base stations can not cover the whole area completely, we can always divide the area into smaller subareas and place more base stations.

# Chapter 4

# TDOA: Time Difference of Arrival Scheme

In this section, we propose TPS, OUT time-based positioning scheme for outdoor wireless sensor networks. This scheme consists of two steps. The first step detects the time difference of signal arrival times from three base stations. We transform these time differences in to range differences from the sensor to the base stations. In the second step, we perform trilateration to transform these range estimates into coordinates.

## 4.1 A Time –Based Location Detection Scheme

Given the locations $(x_a,y_a)$, $(x_b,y_b)$, and $(x_c,y_c)$ of base stations A, B, and C, respectively, we are going to determine the location $(x,y)$ of sensor S, as shown in Fig. 7. Let *v* be the speed of RF beacon signals from A, B, and C. Let $d_{ab}$ be the distance between base stations A and B and $d_{ac}$, be the distance between base stations A and C. Thus $\boldsymbol{d_{ab}} = \sqrt{(x_a - x_b)^2 + (y_a - y_b)^2}$ and $\boldsymbol{d_{ac}} = \sqrt{(x_a - x_c)^2 + (y_a - y_c)^2}$ Let $d_{sa}$, $d_{sb}$, $d_{sc}$ be the unknown distances from *S* to A, B, and C respectively. Our time-based location detection scheme TPS consists of two steps.

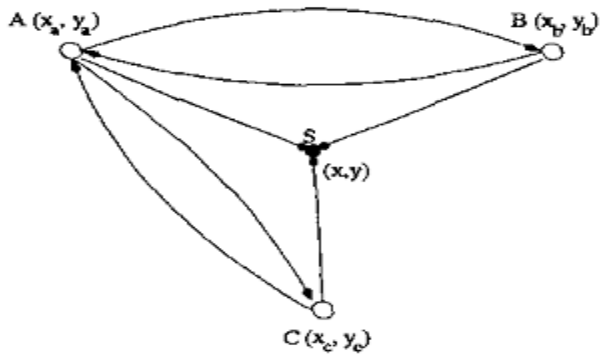


Fig. 7. Sensor *S* will measure TDoA of beacon signals from base stations A. B. and C locally. S *also* will receive the turn-around delay information from B and *C* .B's transmission will start after it receives A s beacon signal, while C's transmission will start after it receives both A and B's beacon signals. This procedure will be repeated once every *T* seconds.

## Step 1: Range Detection.

Let A be the master base station, which will initiate a beacon signal every $T$ seconds. Each beacon interval begins when A transmits a beacon signal. Consider any beacon interval $i$, at times $t^i_1, t^i_b, t^i_c$, sensor S, base stations B and C will all receive A's beacon signal respectively. At time $t^{i'}_b$, which is $\geq t^i_b$, $B$ will reply to A with a beacon signal conveying information $t^{i'}_b - t^i_b = \Delta t^i_b$. This signal will reach $S$ at time $t^i_2$. After receiving beacon signals from both A and B, at time $t^{i'}_c$, C will reply to A with a beacon signal conveying information $t^{i'}_c - t^i_c = \Delta t^i_c$. This signal will reach $S$ at time $t^i_3$. Based on triangle inequality, $t^i_1 < t^i_2 < t^i_3$. Let $\Delta t^i_1 = t^i_2 - t^i_1$, $\Delta t^i_2 = t^i_3 - t^i_1$, we obtain

$$d_{ab} + d_{sb} - d_{sa} + v.\Delta t^i_b = v.\Delta t^i_1 \quad (1)$$

$$d_{ac} + d_{sc} - d_{sa} + v.\Delta t^i_c = v.\Delta t^i_2 \quad (2)$$

which gives

$$d_{sb} = d_{sa} + v.\Delta t^i_1 - d_{ab} - v.\Delta t^i_b = d_{sa} + k^i_1 \quad (3)$$

$$d_{sc} = d_{sa} + v.\Delta t^i_2 - d_{ac} - v.\Delta t^i_c = d_{sa} + k^i_2 \quad (4)$$

Where $d_{sa}$, $d_{sb}$ and $d_{sc}$, are positive real numbers and

$$k^i_1 = v.\Delta t^i_1 - v.\Delta t^i_b - d_{ab} \quad (5)$$

$$k^i_2 = v.\Delta t^i_2 - v.\Delta t^i_c - d_{ac} \quad (6)$$

Averaging $k^i_1$ and $k^i_2$ over I intervals gives

$$k_1 = \frac{V}{I}[\sum_{i=1}^{I}(\Delta t^i_1 - \Delta t^i_b)] - d_{ab} \quad (7)$$

$$k_2 = \frac{V}{I}[\sum_{i=1}^{I}(\Delta t^i_2 - \Delta t^i_c)] - d_{ac} \quad (8)$$

We are going to apply trilateration with $k_1$ and $k_2$ to compute coordinates $(x,y)$ for sensor S in the next step.

## Remarks:

**(i)** All arrival times are measured locally. In other words, $t_1, t_2, t_3$ are measured based on sensor S's local timer; $t^{i}_{b}$ and $t^{i'}_{b}$ are based on B's local timer and known system delays; while $t^{i}_{c}$, and $t^{i'}_{c}$ are based on C's local timer and known system delays. There is no global synchronization.

**(ii)** We require A to periodically initiate the beacon signal transmission for two reasons.

**First**, averaging $k^{i}_{1}$ and $k^{i}_{2}$ over multiple beacon intervals helps to decrease the measurement error. The number of beacon intervals $I$ can be a trade-off between potential accuracy improvement and power consumption.

**Second**, sensors may sleep to save energy; or they may be deployed at different times; or they may move during their lifetime. The periodic beacon signals from A and the reply signals from B and C can facilitate location discovery at any time.

## Step 2: Location Computation.

From Eqs. (3), (4), (7) and (8), we have

$$d_{sb} = d_{sa} + k_1 \tag{9}$$

$$d_{sc} = d_{sa} + k_2 \tag{10}$$

Based on trilateration, we obtain three equations with three unknowns $x, y,$ and $d_{sa},$ where $d_{sa} > 0$

$$(x-x_a)^2 + (y-y_a)^2 = d^2_{sa} \tag{11}$$

$$(x-x_b)^2 + (y-y_b)^2 = (d_{sa} + k_1)^2 \tag{12}$$

$$(x-x_c)^2 + (y-y_c)^2 = (d_{sa} + k_2)^2 \tag{13}$$

In the next Subsection, we will show how to compute $x, y$ and $d_{sa}$ efficiently. We will also give the conditions under which the solution set is unique.

## 4.2 An Efficient Solution for Location Detection by Trilateration

Without loss of generality, we assume the three base stations are located at $(0,0)$, $(x_1,0)$, and $(x_2,y_2)$, respectively, where $x_1 > 0$, $y_2 > 0$. In other words, $x_a = y_a = y_b = 0$, $x_b = x_1$, $x_c = x_2$ and $y_c = y_2$.

Let sensor *S* he located at $(x,y)$. Note that we can always transform real positions to this coordinate system through rotation and translation. We want to compute the location for S.

From Eqs.(l1),(l2),and (13), we have

$$x^2 + y^2 = d^2_{sa} \tag{14}$$

$$x^2 - 2xx_1 + x^2_1 + y^2 = d^2_{sa} + 2d_{sa}k_1 + k^2_1 \tag{15}$$

$$x^2 - 2xx_2 + x^2_2 + y^2 - 2yy_2 + y^2_2 = d^2_{sa} + 2d_{sa}k_2 + k^2_2 \tag{16}$$

Subtracting Eq. (14) from Eq.(15), we obtain

$$2x_1x = -2k_1d_{sa} - k^2_1 + x^2_1 \tag{17}$$

Subtracting Eq. (14) from Eq. (16), we obtain

$$2x_2x + 2y_2y = -2k_2d_{sa} - k^2_2 + x^2_2 + y^2_2 \tag{18}$$

Multiplying Eq. (18) with $x_l$ and Subtracting the product of Eq. (17) with $x_2$, we obtain

$$2x_1y_2y = (2k_1x_2 - 2k_2x_1)\, d_{sa} + k^2_1 x_2 - k^2_2 x_1 + x^2_2 x_1 + y^2_2x_1 - x^2_1x_2 \tag{19}$$

Since $\mathbf{x_1 > 0}$, $\mathbf{y_2 > 0}$, Eq. (17) and (19) can be rewritten as

$$x = (-2k_1d_{sa} - k^2_1 + x^2_1)/2x_1 \tag{20}$$

$$y = [(2k_1x_2 - 2k_2x_1)\, d_{sa} + k^2_1 x_2 - k^2_2 x_1 + x^2_2 x_1 + y^2_2x_1 - x^2_1x_2]/2x_1y_2 \tag{21}$$

Substituting Eqs. (20) and (21) into (14), we obtain

$$\alpha d_{sa}^2 + \beta d_{sa} + \gamma = 0 \quad (22)$$

Where

$$\alpha = 4[k_1^2 y_2^2 + (k_1 x_2 - k_2 x_1)^2 - x_1^2 y_2^2] \quad (23)$$

$$\beta = 4[k_1(k_1^2 - x_1^2) y_2^2 + (k_1 x_2 - k_2 x_1)(k_1^2 x_2 - k_2^2 x_1 + x_2^2 x_1 + y_2^2 x_1 - x_1^2 x_2)] \quad (24)$$

$$\gamma = (k_1^2 - x_1^2)^2 y_2^2 + (k_1^2 x_2 - k_2^2 x_1 + x_2^2 x_1 + y_2^2 x_1 - x_1^2 x_2)^2 \quad (25)$$

**Theorem:**

*Eq.(*22) has a unique positive root for $\mathbf{d_{sa}}$, if and only if one of the following three conditions holds

1) $\alpha = 0$, $\beta < 0$, and $\gamma > 0$;
2) $\alpha\gamma < 0$;
3) $\alpha\beta < 0$, $\gamma = \frac{\beta^2}{4\gamma}$,

**PROOF**

We prove the theorem by case study. First, we consider the case where both $\alpha$ and $\beta$ are zero. In this case, (22) is either satisfied by all values of $d$ (when $\gamma = 0$) or violated by every value of $d$ (when $\gamma \neq 0$).

Next we consider the case where $\alpha = 0$ and $\beta \neq 0$. In this case, (22) has a unique root $d_{sa} = -\frac{\gamma}{\beta}$. Since $\gamma \geq 0$, $-\frac{\gamma}{\beta}$ is positive if and only if $\beta < 0$ and $\gamma > 0$. This corresponds to the first condition in the theorem.

In the rest of the proof, we will consider the cases where $\alpha \neq 0$. Consider the case where $\boldsymbol{\alpha\gamma < 0}$. This implies that $\boldsymbol{\gamma > 0}$ and $\boldsymbol{\alpha < 0}$. It also implies that $\boldsymbol{\beta^2 - 4\alpha\gamma > \beta^2}$ .Therefore (22) has a unique positive root, $\boldsymbol{d_{sa} = \frac{-\beta \pm \sqrt{\beta^2 - 4\alpha\gamma}}{2\alpha}}$. This corresponds to the second condition in the theorem.

In the case where $\boldsymbol{4\alpha\gamma > \beta^2}$, the equation does not have any root in the real field.

In the case where $\boldsymbol{0 < 4\alpha\gamma < \beta^2}$, the equation has two roots $\boldsymbol{d^{(1)}_{sa}} = \frac{-\beta+\sqrt{\beta^2-4\alpha\gamma}}{2\alpha}$ and $\boldsymbol{d^{(2)}_{sa}} = \frac{-\beta-\sqrt{\beta^2-4\alpha\gamma}}{o2\alpha}$ which have the same sign.

In the case where $4\alpha\gamma = \beta^2$, the unique root of the equation is $d_{sa} = -\frac{\beta}{2\alpha}$ which is positive if and only if $\beta < 0$. This corresponds to the third condition in the theorem.

Next consider the case where $\gamma = 0$. Note that $\gamma = 0$ implies that $\boldsymbol{k^2_1 = x^2_1}$ which in turn implies that $\boldsymbol{k^2_1 x_2 - k^2_2 x_1 + x^2_2 x_1 + y^2_2 x_1 - x^2_1 x_2 = 0.}$ Therefore $\boldsymbol{\gamma = 0}$ implies that $\boldsymbol{\beta = 0.}$ In this case, the equation does not have a positive root. This completes the proof of the theorem.

Substituting the value of $\boldsymbol{d_{sa}}$ into Eqs. (20) and (21), we will have the coordinates *x* and y for *S.*

In the above solution, we have used the square root function. Note that computing the square root *X* of a positive number *N* only requires a few iterations of Newton's method [24] in the form of $\boldsymbol{X := 0.5 * ( X + N / X )}$ .Our simulation results show that four iterations are sufficient to produce accurate solutions

**Remarks:**

(i)Newton's method converges quadratically, thus solving trilateration functions can be done in a fast fashion.

(ii) Compared to the other location detection methods in literature [17], [32], [33], [l5], our scheme has an important advantage: we improve performance by refining in the first step-averaging time differences over multiple beacon intervals, which involve only simple algebraic operations. Refining through popular strategies like maximum likelihood or minimum mean square require more computation

We note that data collected may have errors. When solving s system of linear equations such as those defined by (20) and (21), solutions are more accurate when the condition number (the condition number of a system of linear equations is the ratio of the largest eigen value over the smallest eigesn value) is small [9]. We note that the condition number of the system of linear

equations (20) and (21) is max $\{\frac{x1}{y2}, \frac{y2}{x1}\}$.When designing the system, it is better to choose the locations of base stations so that the ratio $\frac{x1}{y2}$ is as close to 1 as possible. It is interesting to note that the value of $x_2$ does not affect the condition number of the system. In practice, we may choose the locations of the base stations so that they are sitting at the vertices of an equilateral triangle. In this case, the condition number will be 1.155, which is very close to 1, resulting in a very stable system**.**

To ensure the unique positive solution for $d_{sa}$, it suffices to have $\alpha\gamma < 0$. From Eq. (25), $\gamma > 0$. Thus the sufficient condition is reduced to $\alpha < 0$. That is

$$k^2_1y^2_2 + (k_1x_2 - k_2x_1)2 < x^2_1y^2_2 \quad (26)$$

which gives

$$k^2_1y^2_2 + k^2_1x^2_2 - k^2_2x^2_1 - 2k_1k_2x_1x_2 < x^2_1y^2_2 \quad (27)$$

In our simulation, this condition is satisfied in all cases where sensors are not in close proximity to or behind a base station. Near the base stations (interior to triangle), the solutions for $d_{sa}$ are both positive. If the position that corresponds to our measurements is interior to the triangle,

$d^{(2)}_{sa} = \frac{-\beta-\sqrt{\beta^2-4\alpha\gamma}}{2\alpha}$ is the correct calculation.

Similarly,

B send signal to S and at times $t^i_4$, $t^i_{a2}$, $t^i_{c2}$, sensor S, base stations A and C will all receive B's beacon signal respectively. At time $t^{i'}_{a2}$, which is $\geq t^i_{a2}$, $A$ will reply to B with a beacon signal conveying information $t^{i'}_{a2} - t^i_{a2} = \Delta t^i_b$. This signal will reach *S* at time $t^i_5$. After receiving beacon signals from both B and A, at time $t^{i'}_{C2}$, C will reply to B with a beacon signal conveying information $t^{i'}_{c2} - t^i_{c2} = \Delta t^i_{c2}$. This signal will reach *S* at time $t^i_6$. Based on triangle inequality, $t^i_4 < t^i_5 < t^i_6$.

Let

$,\Delta t^i_3 = t^i_5 - t^i_4,$

$\Delta t^i_4 = t^i_6 - t^4,$

we obtain

$$d_{ab} + d_{sa} - d_{sb} + v.\Delta t^i_{a2} = v.\Delta t^i_3 \quad (28)$$

$$d_{bc} + d_{sc} - d_{sb} + v.\Delta t^i_{c2} = v.\Delta t^i_4 \quad (29)$$

which gives

$$d_{sa} = d_{sb} + v.\Delta t^i_3 - d_{ab} - v.\Delta t^i_{a2} = d_{sb} + k^i_3 \quad (30)$$

$$d_{sc} = d_{sb} + v.\Delta t^i_4 - d_{bc} - v.\Delta t^i_{c2} = d_{sb} + k^i_4 \quad (31)$$

Where $d_{sa}$, $d_{sb}$ and $d_{sc}$, are positive real numbers and

$$k^i_3 = v.\Delta t^i_3 - v.\Delta t^i_{a2} - d_{ab} \quad (32)$$

$$k^i_4 = v.\Delta t^i_4 - v.\Delta t^i_{c2} - d_{bc} \quad (33)$$

Averaging $k^i_3$ and $k^i_4$ over I intervals gives

$$k_3 = \frac{V}{I}[\sum_{i=1}^{I}(\Delta t^i_3 - \Delta t^i_{a2})] - d_{ab} \quad (34)$$

$$k_4 = \frac{V}{I}[\sum_{i=1}^{I}(\Delta t^i_4 - \Delta t^i_{c2})] - d_{bc} \quad (35)$$

We are going to apply trilateration with $k_3$ and $k_4$ to compute coordinates $(x,y)$ for sensor S in the next step.

From (30),(31),(34),(35),(36) we get

$$d_{sa} = d_{sb} + k_3 \quad (36)$$

$$d_{sc} = d_{sb} + k_4 \quad (37)$$

$$x^2 + y^2 = d^2_{sa} = (d_{sb} + k_3)^2 \quad (38)$$

$$(x - x_1)^2 + y^2 = d^2_{sb} \quad (39)$$

$$(x - x_c)^2 + (y - y_c)^2 = d^2_{sc} = (d_{sb} + k_4)^2 \quad (40)$$

From (38),(39),(40) we get

$$x^2 + y^2 = d^2_{sb} + 2\, d_{sb}\, k_3 + k^2_3 \quad (41)$$

$$x^2 - 2xx_1 + x^2_1 + y^2 = d^2_{sb} \quad (42)$$

$$x^2 - 2xx_2 + x^2_2 + y^2 - 2yy_2 + y^2_2 = d^2_{sb} + 2d_{sb}k_4 + k^2_4 \quad (43)$$

Subtracting Eq**.** (42) from Eq.(41), we obtain

$$2x_1x = 2k_3d_{sb} + k^2_3 + x^2_1$$

$$2x_1x - x^2_1 = 2k_3d_{sb} + k^2_3 \quad (44)$$

$$x = (2k_3d_{sb} + k^2_3 + x^2_1) / 2x_1 \quad (45)$$

Subtracting Eq**.** (43) from Eq.(41), we obtain

$$2x_c\, x - x^2_c + 2y_cy - y^2_c = 2\, d_{sb}\, k_3 + k^2_3 - 2d_{sb}k_4 - k^2_4 \quad (46)$$

Multiplying eqs. (44) into $x_c$ and (46) into $x_1$ we obtain

$$2x_1x_c\, x - x^2_1x_c = 2x_c\, k_3d_{sb} + x_ck^2_3 \quad (47)$$

$$2x_1\, x_c\, x - x_1\, x^2_c + 2x_1\, y_cy - x_1\, y^2_c = 2x_1\, k_3\, d_{sb} + x_1\, k^2_3 - 2x_1\, k_4d_{sb} - x_1k^2_4 \quad (48)$$

Subtracting Eq. (47) from Eq. (48), we obtain

$$y = d_{sb}(x_1k_3 - x_1k_4 - x_ck_4) / x_1y_c + (x_1k^2_3 - x_1k^2_4 - x_ck^2_4 + x_1x^2_c + x_1y^2c - x^2_1x_c) / 2x_1y_c \quad (49)$$

Substituting (44) , (49) in (41) we obtain

$$[(2k_3d_{sb} + k^2_3 + x^2_1) / 2x_1]^2 + [d_{sb}(x_1k_3 - x_1k_4 - x_ck_4) / x_1y_c + (x_1k^2_3 - x_1k^2_4 - x_ck^2_4 + x_1x^2_c + x_1y^2c - x^2_1x_c) / 2x_1y_c]^2 = d^2_{sb} + 2k_3d_{sb} + k^2_3 \quad (50)$$

$$\alpha_1 d^2_{sa} + \beta_1 d_{sa} + \gamma_1 = 0 \quad (51)$$

where

$$\alpha_1 = k^2_3y^2_2 + (x_1k_3 - x_1k_4)^2 + (x_2k_4 + x_1k_4)^2 - 2x_1x_2k_3k_4 - x^2_1y^2_2$$

$$\beta_1 = k^3_3y^2_2 + k_3x^2_1y^2_2 + x^2_1k^3_3 - x^2_1k_3k^2_4 - x_1x_2k_3k^2_1 + x^2_1x^2_2k_3 + x^2_1y^2_2k_3 - x^3_1x_2k_3 - x^2_1k^2_3k_4 + x^2_1k^3_4 + x_1x_2k^3_4 - x^2_1x^2_2k_4 - x^2_1y^2_2k_4 + x^3_1x_2k_4 - x_1x_2k^2_3k_4 + x_1x_2k^3_4 + x^2_2k^3_4 - x_1x^3_2k_4 - x_1x_2y^2_2k_4 + x^2_2x^2_1k_4 - 2x^2_1y^2_2k_3$$

$$\gamma_1 = (x_1k^2_3 - x_1k^2_4 - x_2k^2_4 - x_1x^2_2 + x_1y^2_2 - x_2x^2_1)^2 - 4x^2_1y^2_2k^2_3$$

$$d^{(2)}_{sb} = \frac{-\beta_1 - \sqrt{\beta_1{}^2 - 4\alpha_1\gamma_1}}{2\alpha_1}$$

Consider any beacon interval ***i,*** at times $t^i_7$, $t^i_{a3}$, $t^i_{b3}$, sensor S, base stations A and B will all receive C's beacon signal respectively. At time $t^{i'}_{a3}$, which is $\geq t^i_{a3}$, ***A*** will reply to C with a beacon signal conveying information $t^{i'}_{a3} - t^i_{a3} = \Delta t^i_{a3}$. This signal will reach *S* at time $t^i_8$. After receiving beacon signals from both A and C, at time $t^{i'}_{b3}$, B will reply to C with a beacon signal conveying information $t^{i'}_{b3} - t^i_{b3} = \Delta t^i_{b3}$. This signal will reach *S* at time $t^i_9$. Based on triangle inequality, $t^i_7 < t^i_8 < t^i_9$.

Let $\Delta t^i_5 = t^i_8 - t^i_7$,

$\Delta t^i_6 = t^i_9 - t^i_7$, we obtain

$$d_{ac} + d_{sa} - d_{sc} + v.\Delta t^i_{a3} = v.\Delta t^i_5 \quad (52)$$

$$d_{bc} + d_{sb} - d_{sc} + v.\Delta t^i_{b3} = v.\Delta t^i_6 \quad (53)$$

Which gives

$$d_{sa} = d_{sc} + v.\Delta t^{i}_{5} - d_{ac} - v.\Delta t^{i}_{a3} = d_{sc} + k^{i}_{5} \quad (54)$$

$$d_{sb} = d_{sc} + v.\Delta t^{i}_{6} - d_{bc} - v.\Delta t^{i}_{b3} = d_{sc} + k^{i}_{6} \quad (55)$$

Where $d_{sa}$, $d_{sb}$ and $d_{sc}$, are positive real numbers and

$$k^{i}_{5} = v.\Delta t^{i}_{5} - v.\Delta t^{i}_{a3} - d_{ac} \quad (56)$$

$$k^{i}_{6} = v.\Delta t^{i}_{6} - v.\Delta t^{i}_{b3} - d_{bc} \quad (57)$$

Averaging $k^{i}_{5}$ and $k^{i}_{6}$ over I intervals gives

$$k_{5} = \frac{V}{I}[\sum_{i=1}^{I}(\Delta t^{i}_{5} - \Delta t^{i}_{a3})] - d_{ac} \quad (58)$$

$$k_{6} = \frac{V}{I}[\sum_{i=1}^{I}(\Delta t^{i}_{6} - \Delta t^{i}_{b3})] - d_{bc} \quad (59)$$

We are going to apply trilateration with $k_5$ and $k_6$ to compute coordinates $(x,y)$ for sensor S in the next step.

From (54),(55),(58),(59) we obtain

$$d_{sa} = d_{sc} + k_{5} \quad (60)$$

$$d_{sb} = d_{sc} + k_{6} \quad (61)$$

$$x^2 + y^2 = d^2_{sa} = (d_{sc} + k_5)^2 \quad (62)$$

$$(x - x_1)^2 + y^2 = d^2_{sb} = (d_{sc} + k_6)^2 \quad (63)$$

$$(x - x_2)^2 + (y - y_2)^2 = d^2_{sc} \quad (64)$$

From (62),(63),(64) we obtain

$$x^2 + y^2 = d^2_{sc} + 2\, d_{sc}\, k_5 + k^2_5 \quad (65)$$

$$x^2 - 2xx_1 + x^2_1 + y^2 = d^2_{sc} + 2\, d_{sc}\, k_6 + k^2_6 \quad (66)$$

$$x^2 - 2xx_2 + x^2_2 + y^2 - 2yy_2 + y^2_2 = d^2_{sc} \quad (67)$$

Subtracting Eq**.** (65) from Eq.(66), we obtain

$$2x_1x = -2k_6d_{sc} + 2k_5d_{sc} - k^2_6 + k^2_5 + x^2_1 \quad (68)$$

Subtracting Eq**.** (67) from Eq.(65), we obtain

$$2x_2\, x - x^2_2 + 2y_2y - y^2_2 = 2\, k_5d_{sc} + k^2_5 \quad (69)$$

Multiplying eqs. (68) into $x_2$ and (69) into $x_1$ we obtain

$$2x_1x_2\, x = -2k_6x_2d_{sc} + 2k_5x_2d_{sc} - x_2k^2_6 + x_2k^2_5 + x_2x^2_1 \quad (70)$$

$$2x_1x_2x + 2x_1y_2y = 2x_1k_5d_{sc} + x_1k^2_5 + x_1x^2_2 + x_1y^2_2 \quad (71)$$

From eq. (68) we obtain

$$x = [\, d_{sc}\,(2k_5 - 2k_6) + k^2_5 - k^2_6 + x^2_1]/2x_1 \quad (72)$$

Subtracting Eq. (70) from Eq. (71), we obtain

$$y = d_{sc}(x_1k_5 + x_2k_6 - x_2k_5)\,/x_1y_2 + (x_1k^2_5 + x_1x^2_2 + x_1y^2_2 + x_2k^2_6 - x_2k^2_5 - x_2x^2_1)/2x_1y_2 \quad (73)$$

Substituting (72) , (73) in (65) we obtain

$$[(d_{sc}(2k_5 - 2k_6) + k^2_5 - k^2_6 + x^2_1)/2x_1\,]^2 + [d_{sc}(x_1k_5 + x_2k_6 - x_2k_5)/x_1y_2 + (x_1k^2_5 + x_1x^2_2 + x_1y^2_2 + x_2k^2_6 - x_2k^2_5 - x_2x^2_1)/2x_1y_2]^2 = d^2_{sc} + 2d_{sc}k_5 + k^2_5 \quad (74)$$

$$\alpha_2 d^2_{sc} + \beta_2 d_{sc} + \gamma_2 = 0 \quad (75)$$

Where

$$\alpha_2 = y^2_2 k^2_5 - 2y^2_2 k_5 k_6 + y^2_2 k^2_6 + x^2_1 k^2_5 + x^2_2 k^2_6 + x^2_2 k^2_5 - 2x_1 x_2 k_5 k_6 + 2x^2_2 k_5 k_6 - 2x_1 x_2 k^2_5 - x^2_1 y^2_2$$

$$\beta_2 = y^2_2 k^3_5 - y^2_2 k_6 k^2_5 - y^2_2 k_5 k^2_6 + y^2_2 k^3_6 + y^2_2 x^2_1 k_5 - x^2_1 y^2_2 k_6 + x^2_1 k^3_5 + x_1 x_2 k_6 k^2_5 - x_1 x_2 k^3_5 + x^2_1 x^2_2 k_5 + x_1 x^3_2 k_6 - x_1 x^3_2 k_5 + x^2_1 y^2_2 k_5 + x_1 x_2 y^2_2 k_6 - x_1 x_2 y^2_2 k_5 + x_1 x_2 k_5 k^2_6 + x^2_2 k^3_6 - x^2_2 k_5 k^2_6 - x_1 x_2 k^3_5 - x^2_2 k^2_5 k_6 + x^2_2 k^3_5 - x^3_1 x_2 k_5 - x^2_2 x^2_1 k_6 + x^2_2 x^2_1 k_5 - 2x^2_1 y^2_2 k_5$$

$$\gamma_2 = (x_1 k^2_5 + x_1 x^2_2 + x_1 y^2_2 - x_2 k^2_5 + x_2 k^2_6 - x_2 x^2_1)^2 - 4x^2_1 y^2_2 k^2_5$$

$$d^{(2)}_{sc} = \frac{-\beta_2 - \sqrt{\beta_2{}^2 - 4\alpha_2 \gamma_2}}{2\alpha_2}$$

# Chapter 5

# Theoretical Performance Analysis

The trilateration equations (11), (12). and (13) determine coordinates ***(x,y)*** for sensor *S* based on the measured values $k_1$ and $k_2$**.** The inaccuracies of $k_1$ and $k_2$ cause sensor position errors. From Eqs. (7) and (8). $k_1$ and $k_2$ are the averaged results over ***I*** bcacon intervals, and based on the Central Limit Theorem, $k_1$ and $k_2$ **are** approximately normally distributed when ***I*** is large. Therefore, without loss of generality, may assume $k_1$ and $k_2$ are distributed according to $N(\mu_1,\sigma^2_1)$ and $N(\mu_2, \sigma^2_2)$**,** respectively. In this Section, we first give a statistical error analysis of sensor coordinate estimation. We then identify the major sources of errors affecting TPS's location detection accuracy based on the network model described in Section 3

## 5.1Theoretical Error Analysis

To simplify the elaboration, we consider the case when base stations A, B, and C are located at (0, 0), *(R*,0), and (0,R ***)*** **,**respectively. This base station placement corresponds to condition number 1**,** which results in the most stable system. To further simplify the analysis, we consider the case when *S* is equidistant to any base station. The general case can be analyzed similarly. In our case, it is reasonable to assume $\mu_1 = \mu_2 = 0$, and thus $k_1 / R \approx 0$, $k_2 / R \approx 0$. To facilitate our analysis, **we** further assume that $k_1$ and $k_2$ are independent. (In general, one can introduce correlation between $k_1$ and $k_2$**.)** Plugging $x_1 = R$**,** $x_2 = 0$**,** and $y_2 = R$ into Eqs. (23), (24), and (25), and simplifying the solution to Eq. (22) by approximating $k^2_1/R^2$ and $k^2_2/R^2$with 0, we end up with

$$d_{sa} \approx \frac{\sqrt{2R^2+2k_1k_2}}{2} - (\frac{k_1+k_2}{2}) \tag{76}$$

Substituting the above into Eq. (20) yields

$$x \approx \frac{R}{2} + \frac{k_1 k_2}{2R} - \frac{k_1}{2}\sqrt{2 + \frac{2k_1k_2}{R^2}} \tag{77}$$

Now replacing $(k_1k_2)/R_2 = (k_1/R)(k_2/R)=0$ we obtain

$$x \approx \frac{R}{2} + \frac{k_1 k_2}{2R} - k_1\sqrt{\frac{1}{2}}$$
$$= \frac{R}{2} + k_1 k^*_2 \quad (78)$$

Where $k^*_2 = \frac{k_2}{2R} - \sqrt{\frac{1}{2}}$ Similarly, from Eq. (21) we have

$$Y \approx \frac{R}{2} + \frac{k_1 k_2}{2R} - k_2\sqrt{\frac{1}{2}}$$
$$= \frac{R}{2} + k_2 k^*_1 \quad (79)$$

Where $k^*_1 = \frac{k_1}{2R} - \sqrt{\frac{1}{2}}$

Since ***(x,y)*** is used to estimate the location of S, the error in the estimation must be addressed. There are several ways to do this. The following is a common practice, where the variance of each variable **is** computed and the size of the variance or standard deviation is used **as** a measure of estimation error.

As $\boldsymbol{k_1}$ has a Gaussian distribution with mean $\boldsymbol{\mu_1}$ and variance $\boldsymbol{\sigma^2_1}$, and $\boldsymbol{k_2}$ has a Gaussian distribution with mean $\boldsymbol{\mu_2}$ and variance $\boldsymbol{\sigma^2_2}$,the linear combination $\boldsymbol{k^*_1}$ **;** has a Gaussian distribution with mean $\frac{\mu \mathbf{1}}{2R} - \sqrt{\frac{1}{2}}$ and variance $\frac{\sigma 1^2}{4R^2}$, and $\boldsymbol{k^*_2}$ has a Gaussian distribution with mean $\frac{\mu \mathbf{2}}{2R} - \sqrt{\frac{1}{2}}$ and variance $\frac{\sigma 2^2}{4R^2}$ . Denote by *E (X)*and *V (X)*the mean and variance of a random variable *X* . We have, from Eq. (78).

$$V(x) \approx V(k_1 k^*_2)$$
$$= E(k_1 k^*_2)^2 - [E(k_1 k^*_2)]^2$$
$$= E(k_1 (k^*_2)^2) - [E(k_1 k^*_2)]^2 \quad (80)$$

By the independence between $k_1$ and $k_2$, we have

$$E(k_1 k^*_2) = E(k1)E(k^*_2) \tag{81}$$

$$E(k^2_1(k^*_2)^2) = E(k^2_1)E(k^{*}{}^2_2)$$

$$=[V(k_1) + E(k_1))^2] [V(k^*_2) + E(k^*_2))^2] \tag{82}$$

Therefore substitution gives

$$V(x) \approx V(k_1) [E(k^*_2)]^2 + V(k^*_2) [E(k_1)]^2 + V(k_1) V(k^*_2)$$

$$= \sigma^2_1 (\frac{\mu 2}{2R} - \sqrt{\frac{1}{2}})^2 + \frac{\sigma 2^2}{4R^2} \mu^2_1 + \sigma^2_1 \frac{\sigma 2^2}{4R^2}$$

$$= \frac{\sigma 1^2 \mu 2^2 + \sigma 2^2 \mu 1^2 + \sigma 1^2 \sigma 2^2}{4R^2} + \sigma^2_1 (\frac{1}{2} - \frac{\mu 2}{R} \sqrt{\frac{1}{2}})$$

Since $\mu_1 = \mu_2 = 0$, the above reduces to

$$V(x) \approx \frac{\sigma_1{}^2}{2} + \frac{\sigma_1{}^2 \sigma_2{}^2}{4R^2}$$

$$= \frac{\sigma_1{}^2}{2} (1 + \frac{\sigma_2{}^2}{4R^2}) \tag{83}$$

Similarly, we have

$$V(y) \approx V(k^*_1) [E(k_2)]^2 + V(k_2) [E(k^*_1)]^2 + V(k^*_1) V(k_2)$$

$$= \frac{\sigma 1^2 \mu 2^2 + \sigma 2^2 \mu 1^2 + \sigma 1^2 \sigma 2^2}{4R^2} + \sigma^2_2 (\frac{1}{2} - \frac{\mu 1}{R} \sqrt{\frac{1}{2}})$$

$$= \frac{\sigma_2{}^2}{2} + \frac{\sigma_1{}^2 \sigma_2{}^2}{4R^2}$$

$$= \frac{\sigma_2{}^2}{2} (1 + \frac{\sigma_1{}^2}{4R^2}) \tag{84}$$

From the above analysis, we have the following observations.

**First,** the variance of both ***x*** and y depend on the variances of $k_1$ and $k_2$.

**Second,** the variance of $k_1$contributes more to that of **x** than the variance of $k_2$**;** And the variance of $k_2$ contributes more to that of y than the variance of $k_1$.

**Third,** when ***R*** is large, $V(x) \approx \frac{\sigma_1^2}{2}$, $V(y) \approx \frac{\sigma_2^2}{2}$, showing that the variance of ***x*** is dependent on that of $k_1$ while the variance of y is dependent on that of $k_2$**.**

**Fourth,** if $\sigma_1^2 = \sigma_2^2$**;,** the variances of ***x*** and y can be treated the same in practice.

We note that the above discussion is based only on the first two moments of the random variables $k_1$ and $k_2$**.** We have not taken advantage of the normality assumption of these two variables. In fact, with additional normality **as**sumption on $k_1$ and $k_2$**,** we can obtain approximations to the distributions of x and y. For example, since $k_1$ and $k_2$are independent, the CDF $P(x \leq \alpha)$ of ***x*** can he approximated by (for any real number $\alpha$s).

$$\iint_{\xi\eta \leq \alpha - R/2} \frac{R}{\pi\sigma_1\sigma_2} \exp\{-\frac{1}{2} f(\xi, \eta)\} d\xi d\eta,$$

Where

$$\begin{aligned} f(\xi, \eta) &= \left(\frac{\xi - \mu_1}{\sigma_1}\right)^2 + \left(\frac{2R\eta - \mu_2 + \sqrt{2R^2}}{\sigma_2}\right)^2 \\ &= \left(\frac{\xi}{\sigma_1}\right)^2 + R^2 \left(\frac{2\eta + \sqrt{2}}{\sigma_2}\right)^2 \\ &= \left(\frac{\xi}{\sigma_1}\right)^2 + 2R^2 \left(\frac{1 + \sqrt{2}\eta}{\sigma_2}\right)^2 \end{aligned} \tag{87}$$

The above results will help us to explain simulation results. In our simulation study (Section 6), we consider the cases when the errors of TDoA measurements at the sensor are normally distributed or uniformly distributed. The variance of TDoA measurements determines the variances of $k_l$ and $k_2$ . Simulation results show that position error strongly depends on the variance of TDoA measurements.

## 5.2 Sources of Errors

There are three major sources of errors for our time based location detection scheme: the receiver system delay, the wireless multipath fading channel, and the non-line-of-sight (NLOS) transmission. The receiver system delay is the time duration from which the signal hits the receiver antenna until the signal is decoded accurately by the receiver. This time delay is determined by the receiver electronics. Usually it is constant or varies in very small scale when the receiver and the channel is free from interference. This system delay can he predetermined and can be used to calibrate the measurements. For example, base stations B and C can always eliminate the system delay from $\Delta t^i_b$ and $\Delta t^i_c$ before these values are conveyed to the sensors in their reply messages to A's beacon signal. Meanwhile, as $\Delta t^i_1$ and $\Delta t^i_2$; arc measured by one sensor, the effect of receiver system delay may cancel out. Thus in our model, if base stations B and C can provide precise a priori information on receiver system time delay, their effect will be negligible.

The wireless multipath fading channel will greatly influence the location accuracy of any location detection system. Major factors influencing multipath fading [29] include multipath propagation, speed of the receiver, speed of the surrounding objects, and the transmission signal bandwidth. Multipath propagation refers to the fact that a signal transmitted from the sender can follow a multiple number of propagation paths to the receiving antenna. In our system, the performance is not affected by the speed of the receivers since all sensors and base stations are stationary. However, a moving tank in the surrounding area can cause interference.

There are two important characteristics of multipath signals. First, the multiple non-direct path signals will always arrive at the receiver antennae latter than the direct path signal, as they must travel a longer distance. Second, in LOS transmission model, non-direct multipath signals will normally be weaker than the direct path signal, as some signal power will be lost from scattering. If NLOS exists, the non-direct multipath signal may be stronger, as the direct path is hindered in some way. Based on these characteristics, scientists can always design more sensitive receivers to lock and track the direct path signal. For example, multipath signals using a pseudo-random code arriving at the receiver later than the direct path signal will have negligible effects on a

high-resolution DS-BPSK receiver [4]. Our location detection scheme mitigates the effect of multipath fading by measuring TDoA over multiple beacon intervals. TDoA measurements have been very effective in fading channels, as many detrimental effects caused by multipath fading and processing delay can be cancelled [5].

Another factor related to wireless channels that causes location detection errors is NLOS transmission. To mitigate NLOS effects, base stations can be placed well above the surrounding objects such that there are line-of-sight transmission paths among all base stations and from base stations to sensors.

In the next section, we are going to study the performance of our TPS positioning scheme over fading channels. We will consider the inaccuracy of TDoA information measured at sensors only. The sources of errors under consideration include multipath fading and NLOS. Thus we are going to assume the TDoA measurements are either normally distributed or uniformly distributed. These assumptions are popular in literature for TDoA measurements [5], [17] in fading channels.

# Chapter 6

# Simulation

Eqs. ( 11), (12), and (13) compute coordinates *x* and y for sensor *S* based on $\boldsymbol{k_1}$ and $\boldsymbol{k_2}$, which are determined by the time-related values *at* the sensor *(*$\Delta t^i_1$ and $\Delta t^i_2$) and base stations B *(*$\Delta t^i_b$*)*and C *(*$\Delta t^i_c$*)* over beacon interval I (see Eqs. (7) and (8)). Thus the errors of *x* and y result from the measuring errors of $\Delta t^i_1$, $\Delta t^i_2$, $\Delta t^i_b$, and $\Delta t^i_c$. In this simulation, we assume the measuring errors of $\Delta t^i_b$, and $\Delta t^i_c$ are negligible. This is reasonable, as we can always take possible measures *(see* Subsection 5-2) to decrease the measuring errors of base stations when the number of base stations is small (only 3 in our case). For example, base stations can be placed well above the surrounding objects to avoid multipath fading and NLOS transmission, and the system delay can be predetermined to calibrate the ToA measurements. (In this case, the sensor network resides in a 3-dimensional space. TPS needs to be modified accordingly.) On the other hand, Eqs. (7) and (8) tell us that the measuring error of $\Delta t^i_b$ ( $\Delta t^i_c$) plays the same role as that of $\Delta t^i_1$ ( $\Delta t^i_2$) in the computation of $\boldsymbol{k_1}$ $\boldsymbol{(k_2)}$**.** Thus in our simulation study, we only consider the measuring errors of *(*$\Delta t^i_1$ and $\Delta t^i_{2)}$, which are termed *TDoA* measuring errors in the following description. We will study the influence of *I* and $\sigma^2$ upon position error. Where *I* is the number of beacon intervals used to compute $\boldsymbol{k_1}$ and $\boldsymbol{k_2}$, $\sigma^2$ is the variance of the TDoA measuring error.

We use Matlab to code TPS. This tool provides procedures to generate normally distributed and uniformly distributed random numbers. Measure distance from time delay and velocity of wave. We use the sqrt function in Matlab. Take 10 trials and generate position of source. Generate distances from trails and use the sqrt function in Matlab and we generate the signals for each sensor and determine the position of sensor. We show the true position and estimated position of the sensor. Finally we use time delay function for output that shows in figure 8 the simulation of true position and estimated position of sensors.

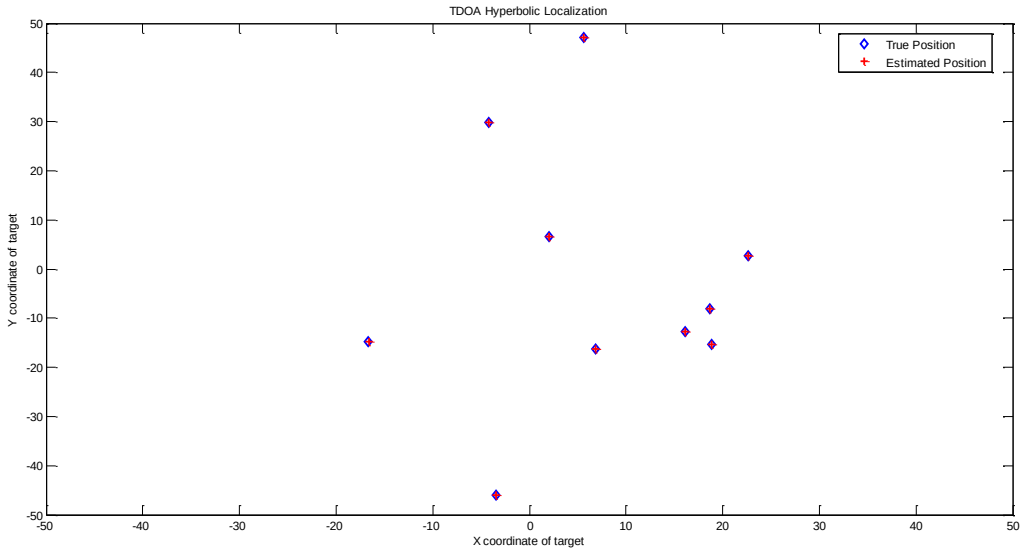


Fig 8: 3D Simulation of True position and Estimated position of Sensors

We first check the correctness of our scheme. In this simulation, no measuring errors are introduced. Base station A is the master base station. We randomly place sensors within the open area formed by the acute angle $\angle BAC$, as shown in Fig. 5. This area is termed *feasible area.* We found that sensors close to the base stations may have two computed locations: one within the feasible area, and one outside. This is because Eq. (22) generates two positive roots for $d_{sa}$. But if we throw away the solution that is outside the feasible area, we can always compute the location for each sensor correctly (uniquely). Thus in the following simulation, we only consider the solutions that are within the open area formed by $\angle BAC$. This is reasonable, as (77) and (78) we determine in equation (77) and (78), the position of unknown sensor S. $\boldsymbol{d_{sa}} = \frac{-\beta-\sqrt{\beta^2-4\alpha\gamma}}{2\alpha}$, $\boldsymbol{d_{sb}} = \frac{-\beta_1-\sqrt{\beta_1{}^2-4\alpha_1\gamma_1}}{2\alpha_1}$, $\boldsymbol{d_{sc}} = \frac{-\beta_2-\sqrt{\beta_2{}^2-4\alpha_2\gamma_2}}{2\alpha_2}$ are the distance of S from A,B and C respectfully.

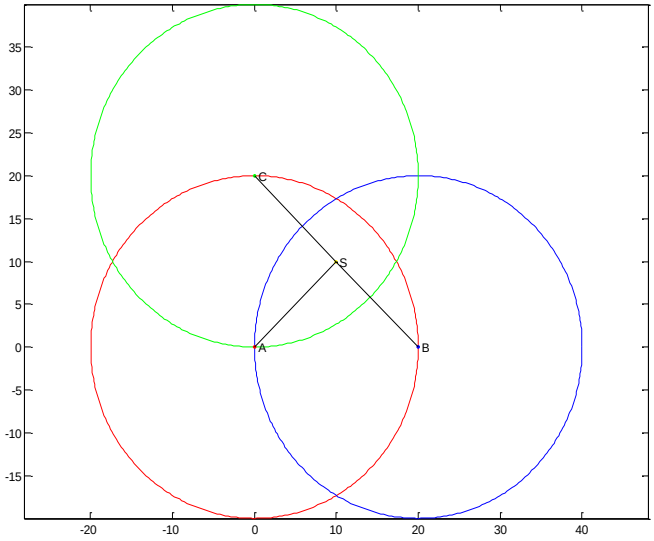


Fig 9: Determination the position of sensor by Trilateration

Fig 9 illustrates the determination the position of sensor by Trilateration. In Figure 9 the three base station positions are (0,0), (20,0) and (0,20).

# Chapter 7

# Conclusion

In this paper, we presented TPS, a time based positioning scheme for outdoor sensor networks. This is a time-based localization scheme that uses only short-range beacons. This scheme is superior to existing systems in many aspects such as computation overhead and scalability. As our scheme requires no time synchronization in the network and minimal extra hardware in sensor construction, thus the scheme is not expensive. The scheme has the strict requirement that the base stations should be able to reach all the sensor nodes in the network. To evaluate the performance of TPS, we conduct both theoretical analysis and simulations, our scheme is simple and effective and practical for location discovery.

# Chapter 8

# Future Detections

Since the proposed method is designed with detection accuracy as a high priority, extension of the method to a large-scale data set requires a significant improvement of the computational complexity of the proposed method. Toward this end, we could benefit from an efficient searching method .These aspects of the work are the subject of ongoing research.

# Reference

[1] C.-Y. Chong, S. Kumar, Sensor networks: evolution, opportunities, and challenges, Proceedings of the IEEE 91 (8) (2003) 1247–1256.

[2] T.E. Biedka, J.H. Reed, B.D. Woerner, Direction finding methods for CDMA systems, in: Thirteenth Asilomar Conference on Signals, Systems and Computers, vol. 1,1996, pp. 637–641.

[3] D.W. Bliss, K.W. Forsythe, Angle of arrival estimation in the presence of multiple access interference for CDMA cellular phone systems, in: Proceedings of the 2000 IEEE Sensor Array and Multichannel Signal Processing Workshop, 2000, pp. 408–412.

[4]J.J Caffery, Ir and G. L. Stiiber, Overview of Radiolocation in CDMA Cellular Systems, IEEE Comunkarions Magazine. pp. 38-45. 1998.

[5] J.J. Caffery, Jr and G. L. Stiiber, Subscriber Location in CDMA Cellular Networks, IEEE Transacfionson VehicularTechnology, Vol. 47, No. 2,pp. 406416, May 1998.

[6] D. Koks, Numerical calculations for passive geolocation scenarios, Tech. Rep. DSTO-RR-0000, 2005.

[7] T. Rappaport, J. Reed, B. Woerner, Position location using wireless communications on highways of the future, IEEE Communications Magazine 34 (10) (1996) 33–41.

[8] L. Gird and D. Estrin, Robust Range Estimation Using Acoustic and Multimodal Sensing, IEEIYRSJ I n f e m a t i o d Conference on Inteligenf Robors and Sysrems, pp. 1312-1320,2001.

[9] C.K. Chen, W.A. Gardner, Signal-selective time-difference of arrival estimation for passive location of man-made signal sources in highly corruptive environments. II. Algorithms and performance, IEEE Transactions on Signal Processing 40 (5) (1992) 1185–1197.

[10] I. Ziskind, M. Wax, Maximum likelihood localization of multiple sources by alternating projection, IEEE Transactions on Acoustics, Speech, and Signal Processing 36 (10) (1988) 1553–1560.

[11] L. Jian, B. Halder, P. Stoica, M. Viberg, Computationally efficient angle estimation for signals with known waveforms, IEEE Transactions on Signal Processing 43 (9) (1995) 2154–2163.

[12] B. Halder, M. Viberg, T. Kailath, An efficient non-iterative method for estimating the angles of arrival of known signals, in: The Twenty-Seventh Asilomar Conference on

Signals, Systems and Computers, 1993, pp. 1396–1400.

[13] B.G. Agee, Copy/DF approaches for signal specific emitter location, in: Conference Record of the Twenty-Fifth Asilomar Conference on Signals, Systems and Computers, vol. 2, 1991, pp. 994–999.

[14] R. Schmidt, ‘‘Multiple emitter location and signal parameter estimation, IEEE Transactions on Antennas and Propagation 34 (3) (1986) 276–280.

[15] E.D. Kaplan (Editor). Undersranding GPS: Principles and Applkarions, Artecb House Publishen, 1996. E161 B. Karp and H. Kung, GPSR: Greedy Perimeter Stateless Routing far Wueless Networks, MOBICOM, pp, 243-254.2000.

[16] A. Paulraj, R. Roy, T. Kailath, A subspace rotation approach to signal parameter estimation, Proceedings of the IEEE 74 (7) (1986) 1044–1046.

[17] F. Koushanfar, S. Slijepcevic, M. Potkonjak, and A. SangiovanniViicentelli, Location Discovery in Ad-Hac Wueless Sensor Networks, in Ad Hoc Wireless Networking (editors X . Cheng, X. Huang and D . 2 . Du), pp. 137-173.2003.

[18] A. Barabell, Improving the resolution performance of eigen structure-based direction-finding algorithms, in: IEEE International Conference on Acoustics, Speech, and Signal Processing, vol. 8, 1983, pp. 336–339.

[19] M. Kaveh, A. Bassias, Threshold extension based on a new paradigm for MUSIC-type estimation, in: International Conference on Acoustics, Speech, and Signal Processing, vol. 5, 1990, pp. 2535–2538.

[20] R. Kumaresan, D.W. Tufts, Estimating the angles of arrival of multiple plane waves, IEEE Transactions on Aerospace and Electronic Systems AES-19 (1983) 134–139.

[21] R. Roy, T. Kailath, ESPRIT-estimation of signal parameters via rotational invariance techniques, IEEE Transactions on Acoustics, Speech, and Signal Processing 37 (7) (1989) 984–995.

[22] R. Klukas, M. Fattouche, Line-of-sight angle of arrival estimation in the outdoor multipath environment, IEEE Transactions on Vehicular Technology 47 (1) (1998) 342–351.

[23] C.D. McGillem and T.S. Rappaport, A Beacon Navigation Method for Autonomous Vehicles, IEEE Transactions on VehiculnrTechnology, Vol. 38, No. 3, pp. 132-139, 1989.

[24] Mm. Books On Line, Square Roors by Newfon's Method, http://www mitpress.mitit.edu/sicp/chapferl/~od~9.h~.

[25] A. Nasipuri and K. Li, A Directionality Based Location Discovery Scheme far Wmless Sensor Networks, WSNA'O2,pp. 105- 111,2002.

[26] D. Niculescu, and B. Nath, Ad-Hoc Positioning System (APS), IEEE GlobeCom. 2001. [27] C. Knapp, G. Carter, The generalized correlation method for estimation of time delay, IEEE Transaction on Acoustics, Speech, Signal Processing 24 (4) (1976) 320327.

[28] A. Rao, S. Ratnasamy, C. Papadimitriou, S . Shenker, and I. Stoic% Geographic Routing Without Location Information MOBICOM,pp. 96.108.2003.

[29] T.S. Rappaport Wireless Communications: Principles ond Pracfice,2nd Edition, Prentice Hall, 2002.

[30] S. Gezici, Z. Tian, G. Giannakis, H. Kobayashi, A. Molisch, H. Poor, Z. Sahinoglu, Localization via ultrawideband radios: a look at positioning aspects for future sensor networks, IEEE Signal Processing Magazine 22 (4) (2005) 70–84.

[31] C. Savarese, J. Rabaey, and K. Langendoen, Robust Positioning Algofithms for Dtsstributed Ad-Hoc Wireless Sensor Networks, USENIX fechnicd annual conference, Monterey, CA, pp. 317-328, 2002.

[32] A. Sawides, C.-C. Han and M.B. Srivastava, Dynamic Fine Grained Localization in Ad-Hoc Networks of Sensors, MOBICOM2001,pp. 166-179.2001.

[33] A. Savvides, H. Park, and M. Srivastaw The Bits and Hops of the N-hop Multilateration Primitive for Node Localization Problems, WSNA'O2,Atlanta, GA, pp. 112-121, 2002.

[34] N. Tayem, H.M. Kwon, Conjugate ESPRIT (C-SPRIT), IEEE Transactions on Antennas and Propagation 52 (10) (2004) 2618–2624.

[35] Y. Shang, W. Ruml, Y. Zhang, and M. Fromherz, Localization From Mere Connectivity MOBIHOC, 2003.

[36] S.V. Schell, W.A. Gardner, High-resolution direction finding, Handbook of Statistics 10 (1993) 755–817.

[37] D. McCrady, L. Doyle, H. Forstrom, T. Dempsey, M. Martorana, Mobile ranging using low-accuracy clocks, IEEE Transactions on Microwave Theory and Techniques 48 (6) (2000) 951–958.

[38] G. Carter, Coherence and Time Delay Estimation, IEEE Press, Piscataway, NJ, 1993.

[39] N.B. Priyantha, A. Chakraborty, H. Balakrishnan, The cricket location-support system, in: Proceedings of the Sixth Annual ACM International Conference on Mobile Computing and Networking, 2000, pp. 32–43.

[40] J.-Y. Lee, R. Scholtz, Ranging in a dense multipath environment using an UWB radio link, IEEE Journal on Selected Areas in Communications 20 (9) (2002) 1677–1683.

[41] G. Carter, Time delay estimation for passive sonar signal processing, IEEE Transactions on Acoustics, Speech, and Signal Processing 29 (3) (1981) 463–470.

[42] W.A. Gardner, C.K. Chen, Signal-selective time-differenceof-arrival estimation for passive location of man-made signal sources in highly corruptive environments. I. Theory and method, IEEE Transactions on Signal Processing 40 (5) (1992) 1168–1184.

[43] K. Romer, The lighthouse location system for smart dust, in: Proceedings of MobiSys 2003 (ACM/USENIX Conference on Mobile Systems, Applications, and Services), 2003, pp. 15–30.

[44] N. Bulusu, 1. Heidemann and D. Estrin, GPS-less Low Cost Outdwr LacaBzation for Very Corn. munictions Magazine, Special Issue onNetworking rhe Physicnl World, August 2000

[45] J. Hightower and G. Bomello, Location System for Ubiquitous Compuring, IEEE Compufer,Vol. 34, No. 8, pp. 57-66,2001

[46] K. Langendoen and N. Reijers, Disuibuted Localization in Wueless Sensor Networks: aQuantitative Comparison, unpublished.